Indonesian Physical Review
Volume 08 Issue 03, September 2025
P-ISSN: 2615-1278, E-ISSN: 2614-7904

Non-Invasive Determination of Liquid Diffusion Coefficients Using Laser Beam Deflection and Refractive Index Gradients: A Study on NaCl

Djati Handoko[1*], Affan Hifzhi[2], Arief Sudarmaji[1], Fitria Yunita Dewi[1]
[1] *Department of Physics, Faculty of Mathematics and Sciences, Universitas Indonesia, Depok, Indonesia*
[2] *NSD Division, PT OMRON Electronics, Jakarta, Indonesia*

Corresponding Author's E-mail: djati.handoko@ui.ac.id

Article Info

Article info:
Received: 25-04-2025
Revised: 22-09-2025
Accepted: 29-09-2025

Keywords:
Diffusion coefficient; Refractive index gradient; Wiener; Fick's law; Laser beam deflection

How To Cite:
D. Handoko, A. Hifzhi, A. Sudarmaji, and F. Y. Dewi, "Non-Invasive Determination of Liquid Diffusion Coefficients Using Laser Beam Deflection and Refractive Index Gradients: A Study on NaCl", Indonesian Physical Review, vol. 8, no. 3, p 815-826, 2025.

DOI:
https://doi.org/10.29303/ipr.v8i3.500.

Abstract

This research describes and verifies the creation of a straightforward system for determining liquid diffusion coefficients using the Laser Beam Deflection (LBD) technique for measuring diffusion rates in sodium chloride solutions. The system exploits refractive index gradients that develop during diffusion to produce a detectable laser beam deviation, which is subsequently analyzed to calculate diffusion coefficients. Our experimental setup, which builds on Wiener's original design with several improvements, consists of a laser source with a cylindrical lens, a diffusion cell, and a screen for capturing projected images. We conducted an in-depth analysis of time-dependent measurements (5, 20, and 45 minutes), concentration variations (20/100, 25/100, and 30/100 NaCl/aquades ratios), and geometric configurations (30°, 45°, and 60° tilt angles) and found that the initial diffusion coefficients exhibit time-dependent behavior before stabilizing at approximately $1.48 \times 10^{-5}\ cm^2/s$. *Within the examined range, concentration had a negligible impact on diffusion coefficients, but the geometric orientation had a substantial effect on measurement accuracy, resulting in a measurement error of approximately 3.00% when the configuration was set at 45°. Linear correlations between the natural logarithm of the ratio of the concentration difference to time* $\ln(dn/dy)$, *and the inverse square of the height* $(h-y)^2$, *were found to be consistent with Fick's second law of diffusion under all tested conditions. This non-invasive approach offers a dependable substitute for conventional methods of diffusion measurement, which may be utilised in fields such as solution chemistry, food science, and pharmaceutical formulations.*

Introduction

Determining liquid diffusion coefficients is crucial in a range of scientific and industrial fields, such as chemical engineering, biomedical research, and environmental science. A comprehensive understanding of diffusion dynamics is crucial for improving processes like

mass transport in biological systems, blending solutions, and fabricating materials [1], [2], [3], [4]. Traditional approaches to measuring diffusion coefficients, which include diaphragm cells, interferometry, and nuclear magnetic resonance, have been employed; however, these methods frequently encounter hindrances such as prolonged measurement times, complex setups, and reduced sensitivity under certain conditions [5], [6], [7], [8]. Fick's laws form the fundamental basis for diffusion analysis, but electrolyte diffusion requires more complex theoretical descriptions. The Nernst-Planck equation accounts for electrostatic interactions between ions [9], with the Debye-Hückel theory explaining activity coefficients in ionic solutions at moderate concentrations [10]. The Einstein-Stokes relation links diffusion coefficients to molecular mobility and solution viscosity[11]. Despite the various concentration ranges and measurement timescales used in this research, Fick's second law is the most suitable framework, as confirmed by the linear relationships observed in our $ln(dn/dy)\ vs\ (h-y)^2$ plots.

Non-invasive and highly sensitive optical methods are increasingly being used to study diffusion phenomena in a detailed manner[5], [12] [13]. Within this category, the Laser Beam Deflection approach has proven effective for determining diffusion coefficients by identifying gradients in refractive index within liquid systems [14], [15]. During the diffusion process, a concentration gradient is created by solutes, resulting in spatial variations in refractive index properties, which cause a measurable deflection of the incident laser beam[16]. Researchers can determine highly accurate diffusion coefficients by conducting a sophisticated analysis of the time-dependent deflection patterns, thereby minimizing experimental interference [17], [18]. Current research on laser beam deflection is primarily focused on gas-phase measurements in controlled environments, with limited exploration of its practical applications in liquid phases [14], [15]. Researchers Yao et al. [14] have shown laser spot deflection for measuring hydrogen jet concentrations, but their method relies on custom-built gas handling equipment and is not directly adaptable for use in liquid diffusion systems. Köhler et al. [15] have developed comprehensive methodologies for measuring the Soret coefficient in binary mixtures, but these techniques require complex thermal gradient control systems that may not be practical for routine diffusion coefficient measurements. Existing optical diffusion measurement methods typically involve costly interferometric equipment or have low sensitivity in moderate concentration ranges. The existing gap requires the creation of a simplified, cost-efficient laser beam deflection system tailored for liquid diffusion measurements with increased accuracy and wider usability.

This research developed a straightforward system for measuring a liquid diffusion coefficient based on gradients in refractive index, employing the LBD method with sodium chloride (NaCl) selected as the trial solute. Sodium chloride is commonly utilised in diffusion studies owing to its well-defined physicochemical properties and its significance in industrial and biological contexts [19], [20], [21]. NaCl was selected over other common electrolytes like KCl for several reasons, including the fact that NaCl shows more pronounced refractive index gradients per unit change in concentration, thereby increasing the sensitivity of measurements in laser beam deflection methods. Sodium chloride has significant biological and industrial importance, especially in physiological systems and food processing industries. In addition, it has well-documented physicochemical properties that serve as reliable reference standards for

validating our measurement technique. The system was developed by using the camera to capture reflected beam, to accomplish high precision via laser optics, highly responsive position sensing, and advanced data analysis techniques. Details regarding the experimental setup and data analysis methods employed for calculating diffusion coefficients from laser deflection data will be addressed.

The specific novelty of this research lies in the creation of a simplified laser beam deflection system that is tailored for liquid diffusion measurements, without the need for intricate interferometric equipment. The method offers a systematic examination of geometric optimisation (tilt angle effects) to improve measurement accuracy. A thorough examination of time-dependent behavior is conducted to differentiate measurement errors from genuine physical occurrences and to demonstrate the method's reliability across various concentration levels with a quantitative assessment of errors. Unlike previous studies focused primarily on gas-phase applications or requiring sophisticated thermal control systems, our approach offers a practical, cost-effective alternative for the routine determination of liquid diffusion coefficients, which has potential applications in solution chemistry, food science, and pharmaceutical formulation.

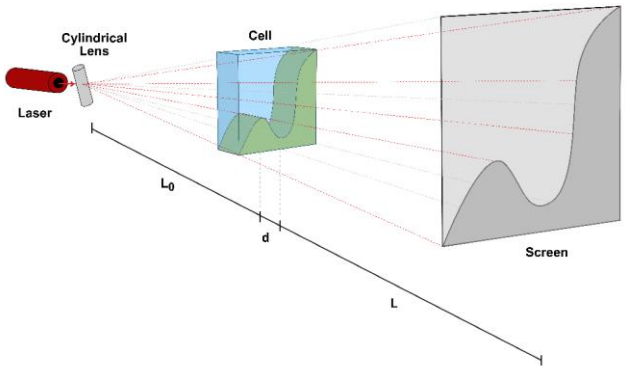

Figure 1. Experimental setup based on Wiener's original design

Experimental Method

The experimental instrument was based on Wiener's original setup, with additional modifications including a laser fitted with a cylindrical lens and a slit, a diffusion cell, and a screen for capturing the projected image. A diagram of the apparatus is included in Figure 1. The laser source was a 650 nm diode laser (red wavelength) with an output power of 5 mW and beam diameter of approximately 2 mm. A laser beam is directed to a cylindrical lens, positioned perpendicularly to the beam and angled 45° relative to the vertical axis. As a consequence, a line perpendicular to the vertical axis at a 45° angle will be cast onto the screen prior to the observation of the sample. The cylindrical lens sends light to a cell situated 20 cm from the lens. The test sample is positioned within a cell with a thickness of 0.8 cm. The light will then pass through the sample and travel to a screen positioned 75 cm from the cell. The screen will display the image produced by the deflection of the sample within the cell.

The sample is prepared by filling the cell with a more concentrated solution, which is an aqueous solution of sodium chloride. A cell was initially filled with a sodium chloride solution, after which distilled water was gradually added and mixed with the sodium chloride within it. A very thin layer, about 0.1 cm thick, develops at the interface between NaCl and distilled water, resulting in a distinct clear boundary. The objective is to generate two interfaces between liquids of different densities and concentrations, which leads to the observed diffusion effects, as shown in Figure 2.

Each measurement session was performed at a temperature of 23 ± 1°C, which was continuously monitored using a digital thermometer. Prior to each experiment, a 30-minute equilibration period was allowed for the diffusion cell and its surrounding environment to reach thermal equilibrium, thereby reducing temperature-induced convection effects. The laboratory environment was kept stable without active temperature control, maintaining a temperature range of ±1°C throughout the measurement periods.

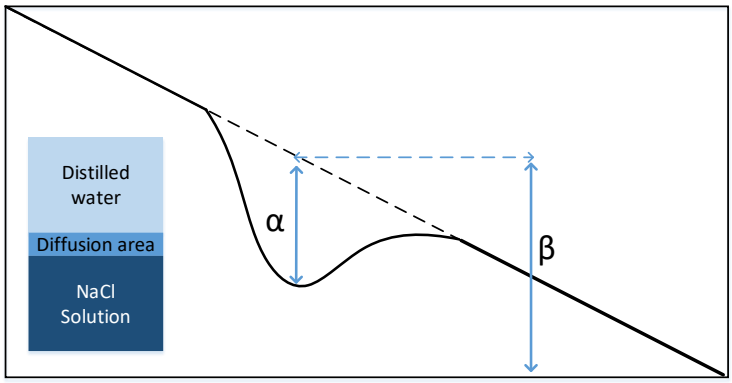

Figure 2. The image preview is displayed on the screen once the test sample is completed. The cellular composition is represented by the blue section. The *a* value directly measures deflection as a departure from a straight line. The vertical position β can be used to calculate *dn/dy* and *Y*i.

As the sample fills the cell, the laser beam's appearance on the screen changes once the thin interface layer within the sample starts to form; at first, it shows a single line tilted at about 45 degrees to the vertical axis, but it later shifts within the area where inter-diffusion occurs. The image shown on the projection screen is illustrated in Figure 2. Using the results that have been obtained, it is possible to determine the α and β values required to proceed with analysing the refractive index gradient profile. The experimental setup's geometric properties allow for the determination of Yi from β via equation (1), and $(dn\ /\ dy)_i$ from α via equation (2), both equations having been derived from optical geometry and Snell's law.

$$Y_i = \frac{\beta L_0}{L_0 + d + L} \tag{1}$$

$$\left(\frac{dn}{dy}\right)_i = \frac{\alpha_i}{dL} \tag{2}$$

Here, a signifies the horizontal deflection angle of the laser beam (in radians), β indicates the vertical position on the projection screen (in mm), *Y*i denotes the corresponding vertical position within the diffusion cell (in mm), h is the height parameter at the position of the

maximum refractive index gradient, d represents the cell thickness (0.8 cm), L is the distance from the cell to the screen (75 cm), and L_0 is the distance from the lens to the cell (20 cm).

However, because the Gaussian curve is not always perfectly fit, we need to calculate value of h (the highest value of $\frac{dn}{dy}$) using simple relations (3):

$$h = \frac{(Y_{i+1}^2 - Y_i^2)\left(\frac{dn}{dy}\right)_i}{Y_i} \tag{3}$$

Furthermore, the diffusion coefficient (D) of NaCl-distilled water based on the slope of the curve by combining simple relations between (4) and (5):

$$ln\left(\frac{dn}{dy}\right) \approx m(h-y)^2 + C \tag{4}$$

$$m = -\frac{1}{4Dt} \tag{5}$$

The calculations were carried out in accordance with Fick's law, supplemented by information presented in previously conducted studies [22], [23], [24].

A diffusion layer develops at the boundary between an aqueous NaCl solution and distilled water, resulting in a varying refractive index which causes the deflection of a laser beam. The image data logger records and saves the deflection curve. In-depth examination has been facilitated by experiments carried out involving time-dependent diffusion, a spectrum of NaCl concentrations, and adjustments made to the laser beam's angle of incidence. All the process was summarized in a flowchart as depicted in Figure 3.

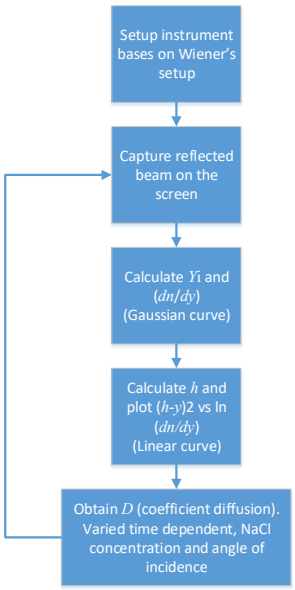

Figure 3. Flowchart experiment

Result and Discussion

The diffusion profile data show the way the refractive index gradients change over time (dn/dy) with respect to (Y_i), at three specific measurement times: 5, 20, and 45 minutes. The

data demonstrate a distinct sequence of changes, with the 5-minute pattern displaying the greatest peak intensity (~1.5 mm^{-1}) and smallest breadth, followed by a steady decrease in peak intensity and widening at 20 minutes (~0.9 mm^{-1}) and 45 minutes (~0.6 mm^{-1}), as illustrated in Figure 4 (a). This pattern matches established diffusion theory and suggests the expected outcome of a diffusion-driven homogenization process, where the initially distinct concentration boundary fades over time, as seen in recent studies of analogous liquid systems[17], [25]. The inset graph illustrates a linear correlation between $ln(dn/dy)$ and $(h-y)^2$, at every measurement point, thereby validating compliance with Fick's second diffusion law as outlined in current studies. The varying gradients across the three data collection points indicate a possible dependence of diffusion behaviour on time, a trend also observed in recent research studies [15], [26]. The overall data quality demonstrates high measurement precision with distinct separation between time intervals, comparable to findings achieved with analogous laser deflection techniques [26]. The consistent peak position at 21-22 mm suggests that the diffusion midpoint remained spatially stable throughout the experiment, thereby supporting the reliability of the experimental setup and measurement approach, as also noted in current studies.

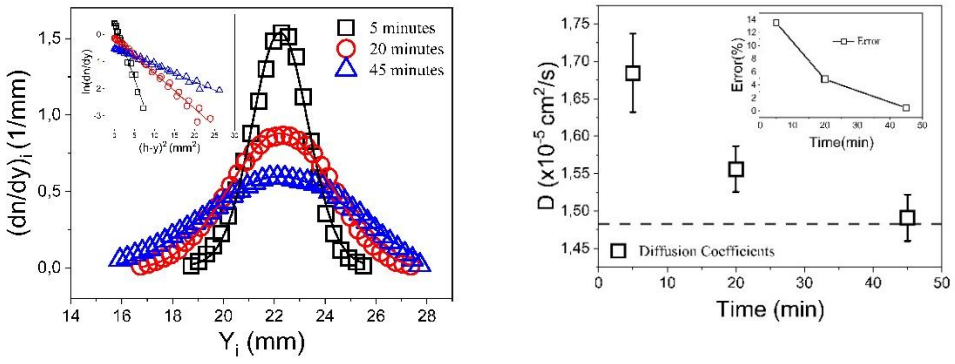

(a) (b)

Figure 4. Time-dependent measurement, on Gaussian response (a) and coefficient diffusion (b).

The diffusion coefficient, denoted as D, displays a marked decline over time. Initially, it measured approximately $1.68 \times 10^{-5}\ cm^2/s$ at 5 minutes. A subsequent decrease was observed to about $1.55 \times 10^{-5}\ cm^2/s$ at 20 minutes. Furthermore, it was found to be approaching $1.49 \times 10^{-5}\ cm^2/s$ by 45 minutes, as illustrated in Figure 4 (b). The system's movement towards a stable point, as shown by the horizontal dashed line at roughly $1.48 \times 10^{-5}\ cm^2/s$, implies that it undergoes temporary diffusion patterns before stabilizing into equilibrium, a process observed in current research on diffusion. The inset indicates a significant reduction in experimental error as measurement time increases, dropping from roughly 13.0% at 5 minutes to 5.00% at 20 minutes and then falling below 1.00% by 45 minutes. This inverse relationship is consistent with established principles of diffusion measurement methodologies, suggesting that longer measurement periods result in more reliable diffusion coefficient values as the system approaches a steady-state condition. The error bars on the main plot provide additional evidence for this trend, revealing significantly narrower

uncertainty ranges at later time points, implying that D's apparent time-dependency could be partly due to measurement limitations at early stages rather than solely reflecting its inherent physical characteristics.

The observed time-dependence of the diffusion coefficient probably results from a mixture of physical processes and measurement errors rather than actual changes in the inherent diffusion coefficient. Initial variations in D may be influenced by residual convection effects and interface instabilities from the sample preparation process during the initial stages (5-20 minutes). As transient effects become less significant, the system eventually reaches a state of pure diffusive transport, leading to stable D values at longer time periods. The reduction in measurement error over time (from 13.0% to less than 1.00%) lends credence to this interpretation, implying that the apparent time dependence is mainly attributed to early-stage measurement limitations rather than fundamental alterations in the diffusion process itself.

A detailed examination is provided in Figure 5(a), which displays gradient profiles of refractive index across different positions in experiments involving diffusion with three distinct concentration ratios. The systematic increase in peak height with concentration ratio indicates that greater initial concentration differences result in steeper refractive index gradients. The Gaussian-shaped distribution profiles in all three cases show consistent diffusion behaviour, unaffected by the magnitude of concentration[20], [27]. The inset graph displays a linear correlation between $ln(dn/dy)$ and $(h-y)^2$ for all three concentration ratios, and exhibits nearly identical slopes across the diverse concentration conditions. The striking similarity implies that the concentration of D's remains unaffected throughout the examined range. The uniformity of data from all sets clearly supports the application of Fick's second law of diffusion and confirms the accuracy of the experimental approach. The symmetrical peaks near position Yi of approximately 17-18 mm suggest that the experimental conditions are well-controlled, allowing for uniform diffusion to occur in both directions from the initial interface. This symmetry provides a solid basis for accurately determining the diffusion coefficient across different concentration gradients [28].

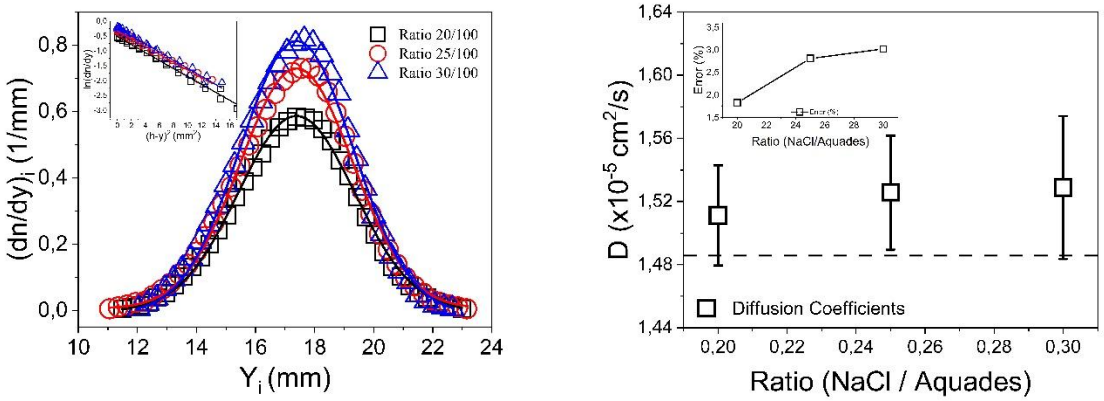

(a) (b)

Figure 5. Illustrates the concentration of NaCl dependent measurement on Gaussian response (a) and coefficient diffusion (b).

The relationship between D and the concentration ratio of NaCl to water at three distinct concentration levels - 0.20, 0.25, and 0.30 - is illustrated in Figure 5(b). The concentration ratio is seen to steadily rise as the concentration increases, beginning at around $1.51 \times 10^{-5}\ cm^2/s$ at a ratio of 0.20, reaching approximately $1.52 \times 10^{-5}\ cm^2/s$ at a ratio of 0.25, and eventually reaching $1.53 \times 10^{-5}\ cm^2/s$ at a ratio of 0.30. The substantial overlap of error bars across all three measurements implies that the observed differences may not be statistically substantial, which indicates that the diffusion coefficient remains relatively consistent across the tested concentration range. The inset graph offers further insight by illustrating the percentage error in relation to concentration ratio, revealing a growing trend of measurement uncertainty at higher concentrations, ranging from approximately 1.70% at a ratio of 0.20 to 2.80% at 0.25, and reaching about 3.00% at 0.30.

The increasing inaccuracy in measurement at higher concentration levels can be attributed to several factors related to ionic interactions and non-ideal solution properties. Debye-Hückel theory asserts that higher ionic concentrations cause heightened electrostatic interactions between ions, which in turn leads to activity coefficient deviations from ideal behaviour. These deviations can lead to non-uniform concentration gradients and potential micro-convection effects which can interfere with the pure diffusion process. Greater differences in concentration can also lead to density-driven convection instabilities at the interface, especially during the initial mixing process, resulting in systematic errors in the measurements of the refractive index gradient. Recent research supports the notion that measurement accuracy generally deteriorates at higher concentration differences because of increased imperfections in solution behavior and potential convection effects that can interfere with pure diffusion processes [28]. The dashed horizontal line at approximately$1.48 \times 10^{-5}\ cm^2/s$ is thought to represent a reference standard or theoretical estimate for the diffusion coefficient, acting as a baseline for evaluating experimental findings and verifying the measurement technique.

In addition, the angular dependence of the spatial derivative of the refractive index as a position function displays characteristic Gaussian distributions with systematic peak shifts at tilt angles of 30°, 45°, and 60°, as illustrated in Figure 6(a). Results from a quantitative analysis show that raising the tilt angle results in a regular leftward shift of the peak position, with the 60-degree configuration exhibiting the greatest movement towards lower Yi values relative to the 30-degree baseline. The inset implies an exponential decay component in the refractive index profile, pointing to a feature of diffusion-mediated gradient formation. The full width at half maximum (FWHM) values rise as the tilt angle is increased, showing an 18.3% greater width for the 60° setup compared to the 30° arrangement. This occurrence can be attributed to increased optical path length and beam divergence effects which become more pronounced at steeper angles, resulting in broader diffusion profiles in projected measurements. Results indicate minimal wavefront distortion across all tilt configurations, implying that robust experimental methodology has been employed despite varying incident angles [29]. The outcomes of these findings have substantial implications for the use of gradient-index optics, where accurate control of refractive index profiles is essential, especially in beam-steering components and optical wave-guides, where sensitivity to angular changes directly affects device performance.

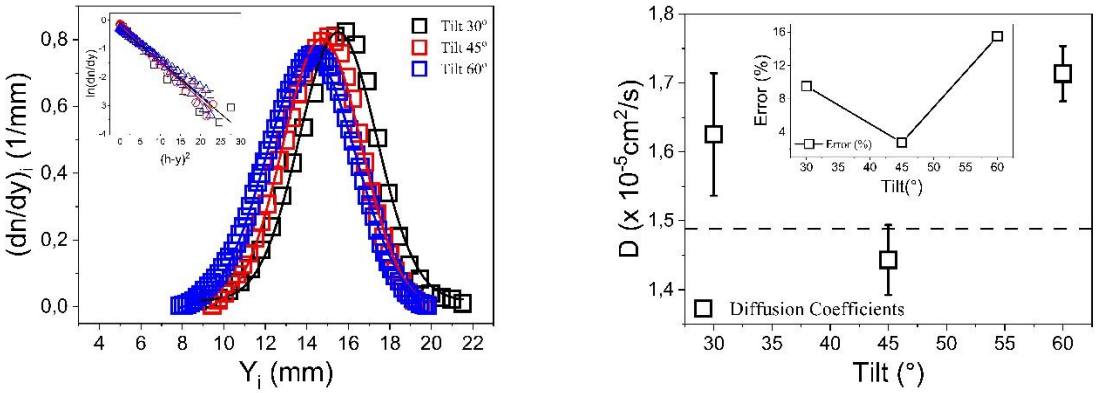

(a) (b)

Figure 6. Gaussian response (a) and diffusion coefficient (b) concerning laser tilt angle variation.

A non-monotonic relationship between D and tilt angle is observed, with corresponding values of approximately$1.62 \times 10^{-5}\ cm^2/s$ at a 30° tilt angle, $1.45 \times 10^{-5}\ cm^2/s$ at a 45° tilt angle, and $1.71 \times 10^{-5}\ cm^2/s$ at a 60° tilt angle, as illustrated in Figure 6(b). The diffusion processes are significantly impacted by the geometric orientation of the setup, with a notable decrease of 15.0% in diffusion rate observed in the 45° configuration compared to the 60° orientation, caused by a more symmetric Gaussian curve resulting. A closer examination of the graph reveals a clear linear relationship between measurement error and the diffusion coefficient, and it appears that achieving the lowest measurement error of approximately 3.00% occurs simultaneously with the diffusion rate at 45°, implying that optimal measurement precision may be achieved at this angle.

Although resulting in a lower absolute diffusion coefficient value, the optimal measurement precision at a 45° tilt angle can be explained by geometric and optical factors. At 45°, the laser beam path achieves the most symmetrical optical geometry in relation to the diffusion cell, thereby reducing aberrations and edge effects that can distort the refractive index gradient measurements. The angle strikes the right balance between its sensitivity to changes in refractive index and its geometric stability. Angles of 30° result in greater path length variations and increased beam walk-off effects, whereas 60° angles could decrease the effective interaction length with the diffusion gradient. The variation in diffusion coefficient values across different angles is probably due to geometric measurement artefacts rather than actual changes in the physical diffusion process, highlighting the significance of standardised measurement geometry for obtaining reliable results.

Study Limitations and Future Directions

Several limitations are evident in this study and should be acknowledged. Initially, only sodium chloride (NaCl) was examined as the test solute, thereby constraining our capacity to evaluate the method's broad applicability across various chemical systems. Next, the concentration range was quite limited at 20.0% - 30.0% NaCl/water ratios, with experiments taking place under isothermal conditions that might not accurately represent real-world scenarios. Currently, the setup necessitates manual sample preparation and visual observation, potentially resulting in operator-dependent variations.

Future research should be expanded to incorporate other significant solute systems, such as KCl for comparison with standard electrolyte studies, glucose and sucrose solutions relevant to food science, and ethanol-water mixtures crucial in pharmaceutical formulations. Furthermore, studying temperature-dependent diffusion behaviour and automating sample handling could increase the technique's flexibility and measurement accuracy. The method's scientific and industrial applications would be further broadened by developing real-time monitoring capabilities and extending it to ternary systems.

Conclusion

This research effectively shows that the LBD method combined with refractive index gradient analysis provides a potent non-invasive method for determining liquid diffusion coefficients in NaCl solutions. Measurements taken over time show that longer diffusion periods yield more stable and precise results, with the diffusion coefficients converging to approximately $1.48 \times 10^{-5}\ cm^2/s$ as equilibrium conditions are approached. Within the studied range of 20/100 to 30/100 NaCl/aquades, variations in concentration had a negligible effect on diffusion coefficients, whereas the geometric setup played a significant role in measurement accuracy, with the 45° tilt angle arrangement resulting in the lowest error rate of approximately 3.00% despite producing the lowest absolute diffusion coefficient value. The linear relationships evident in $ln(dn/dy)$ and $(h-y)^2$, are consistent across all experimental conditions, supporting the system's adherence to Fick's second law of diffusion and thereby validating our methodology. This versatile analytical method has considerable potential applications in various solute-solvent systems beyond NaCl solutions, including pharmaceutical development, environmental monitoring, and materials science, where a precise understanding of mass transport phenomena is crucial for process optimisation and quality control. Research could focus on incorporating extra solutes and refining the geometric setup in order to increase the versatility of this measurement system across wider concentration ranges and more intricate solution settings.

Acknowledgement

The authors would like to express their gratitude to FMIPA Universitas Indonesia for the financial support.

References

[1] D. C. Gomes, V. Geraldes, D. Fegley, and M. A. Rodrigues, "Mutual diffusion of proteins in cold concentration gradients measured by holographic interferometry," *Chem Eng Sci*, vol. 236, Jun. 2021.

[2] J. Shao *et al.*, "Measurements of diffusion characteristics of hydroxyl radical with laser-induced fluorescence at high temperature," *Opt Commun*, vol. 488, Jun. 2021.

[3] G. G. Carandang, R. Nakanishi, and N. Kakuta, "Near-infrared imaging-based diffusion coefficient mapping for acid–base reactions," *Chemical Engineering Journal*, vol. 479, Jan. 2024.

[4] M. Aman, D. Handoko, A. Sudarmaji, Handoyo, and L. Soedarmawan, "Determination of Diffusion Coefficient of Palm Oil in n-Hexane Using Laser Deflection Method and Image Processing," in *IOP Conference Series: Earth and Environmental Science*, Institute of Physics, 2022.

[5] D. Ambrosini and P. K. Rastogi, "Diffusion measurements by optical methods: Recent advances and applications," Dec. 2008. doi: 10.1016/j.optlaseng.2008.08.006.

[6] John. Crank, *The mathematics of diffusion*. Clarendon Press, 1975.

[7] D. Ambrosini, D. Paoletti, and N. Rashidnia, "Overview of diffusion measurements by optical techniques," *Opt Lasers Eng*, vol. 46, no. 12, pp. 852–864, Dec. 2008.

[8] R. Wang, W. Meng, Y. Zhang, D. Li, and X. Pu, "An improved method for measuring the concentration dependence of Fick diffusion coefficient based on Boltzmann equation and cylindrical liquid-core lenses," *International Communications in Heat and Mass Transfer*, vol. 138, Nov. 2022.

[9] B. Illés, B. Medgyes, K. Dušek, D. Bušek, A. Skwarek, and A. Géczy, "Numerical simulation of electrochemical migration of Cu based on the Nernst-Plank equation," *Int J Heat Mass Transf*, vol. 184, Mar. 2022.

[10] L. Sun, Q. Lei, B. Peng, G. M. Kontogeorgis, and X. Liang, "An analysis of the parameters in the Debye-Hückel theory," *Fluid Phase Equilib*, vol. 556, May 2022.

[11] M. Hamada and P. de Anna, "A Method to Measure the Diffusion Coefficient in Liquids," *Transp Porous Media*, vol. 146, no. 1–2, pp. 463–474, Jan. 2023.

[12] L. Sun, W. Meng, and X. Pu, "New method to measure liquid diffusivity by analyzing an instantaneous diffusion image," *Opt Express*, vol. 23, no. 18, p. 23155, Sep. 2015.

[13] L. Wei, X. Pu, and D. Cheng, "Optical measurement of concentration-dependent diffusion coefficient by tracing diffusion image width," *Optik (Stuttg)*, vol. 270, Nov. 2022.

[14] K. Betts, K. Y. Heenkenda, B. Jacome, S. Kim, M. Tovar, and Z. Feng, "Refractive Laser Beam Measuring Diffusion Coefficient of Concentrated Battery Electrolytes," *J Electrochem Soc*, vol. 171, no. 2, p. 020551, Feb. 2024.

[15] Y. Ge *et al.*, "Application and development of optical-based viscosity measurement technology," Oct. 01, 2024.

[16] N. Kumawat, P. Pal, and M. Varma, "Diffractive optical analysis for refractive index sensing using transparent phase gratings," *Sci Rep*, vol. 5, Nov. 2015.

[17] L. Yao *et al.*, "Measurements of concentration distribution of hydrogen jet using deflection of center of the laser spot," *Int J Hydrogen Energy*, vol. 47, no. 83, pp. 35515–35526, Oct. 2022.

[18] W. Köhler, A. Mialdun, M. M. Bou-Ali, and V. Shevtsova, "The Measurement of Soret and Thermodiffusion Coefficients in Binary and Ternary Liquid Mixtures," Sep. 01, 2023.

[19] C. Y. Son and Z. G. Wang, "Ion transport in small-molecule and polymer electrolytes," Sep. 14, 2020.

[20] Y. Ge *et al.*, "Application and development of optical-based viscosity measurement technology," Oct. 01, 2024.

[21] J. Chen *et al.*, "Apparent diffusion coefficient and tissue stiffness are associated with different tumor microenvironment features of hepatocellular carcinoma," *Eur Radiol*, Nov. 2024.

[22] *2017 International Seminar on Sensors, Instrumentation, Measurement and Metrology (ISSIMM) : proceedings : Innovation for the Advancement and Competitiveness of the Nation : Universitas Airlangga, Faculty of Science and Technology, Surabaya, Indonesia, August 25th-26th, 2017*. IEEE, 2017.

[23] L. Soedarmawan, M. Aman, A. Hifzhi, S. Pambudi, A. Sudarmaji, and D. Handoko, "Diffusion coefficient measurement system based on laser beam deflection on liquid: Image and data processing," in *AIP Conference Proceedings*, American Institute of Physics Inc., Nov. 2019.

[24] *2017 International Seminar on Sensors, Instrumentation, Measurement and Metrology (ISSIMM) : proceedings : Innovation for the Advancement and Competitiveness of the Nation : Universitas Airlangga, Faculty of Science and Technology, Surabaya, Indonesia, August 25th-26th, 2017*. IEEE, 2017.

[25] C. D. Costin and R. E. Synovec, "Measuring the transverse concentration gradient between adjacent laminar flows in a microfluidic device by a laser-based refractive index gradient detector." [Online]. Available: www.elsevier.com/locate/talanta

[26] Z. Liu, Y. Cheng, L. Wang, B. Pang, W. Li, and J. Jiang, "Experimental investigation of the constant and time-dependent dynamic diffusion coefficient: Implication for CO2 injection method," *Fuel*, vol. 267, May 2020.

[27] R. Wang, W. Meng, Y. Zhang, D. Li, and X. Pu, "An improved method for measuring the concentration dependence of Fick diffusion coefficient based on Boltzmann equation and cylindrical liquid-core lenses," *International Communications in Heat and Mass Transfer*, vol. 138, Nov. 2022.

[28] A. Bardow, V. Göke, H. J. Koß, K. Lucas, and W. Marquardt, "Concentration-dependent diffusion coefficients from a single experiment using model-based Raman spectroscopy," in *Fluid Phase Equilibria*, pp. 357–366, Feb. 2005.

[29] A. Yurin, G. Vishnyakov, V. Minaev, and A. Golopolosov, "The modified minimum deviation method for measuring the refractive index," *Optik (Stuttg)*, vol. 292, Nov. 2023.